Supplemental Experimental Procedures

Adenoviruses

Adenovirus encoding both FLAG-tagged wild type mouse PPARα and a GFP marker, and an adenovirus encoding GFP alone were gifts from T. C. Leone and D. P. Kelly. The AdPPARα virus is known to result in expression of a protein that transactivates PPARα target genes (Bernal-Mizrachi et al., 2003; Tordjman et al., 2002). The DNA binding domain (DBD) mutant of PPARα was generated by mutating the two highly conserved cysteine residues (Shi et al., 2002) to alanine (C119A, C122A) using site-directed mutagenesis (QuikChange® kit, Stratagene). The DBD mutant was subcloned into the pCMV-TAG1 vector (Stratagene) to acquire a FLAG tag, then shuttled into pAdTrack-CMV vector encoding a GFP marker and recombined with Ad-Easy1 vector. The pAdTrack-CMV and pAdEasy-1 vectors were gifts from the laboratory of B. Vogelstein. Viruses were purified and expanded as described (Bernal-Mizrachi et al., 2003; Tordjman et al., 2002). The presence of GFP in each of the adenoviruses allowed a simple estimation of transduction efficiency. Viruses were administered by slow intravenous infusion at a dose of 8.5×10^{10} PFU, each in a total volume of 200 μl. Livers were rapidly removed on day 4 after injections, a time period noted to produce optimal viral transduction (Bernal-Mizrachi et al., 2003) and FLAG tagged PPARα was isolated.

Quantitative RT-PCR−based Gene Expression

Total RNA was extracted from Hepa 1-6 cells and liver using Trizol (Invitrogen) and treated with DNase I (RNase-free, Roche Molecular Biochemicals). Reverse transcription to cDNA and real-time quantitative PCR were performed using previously published procedures and primer-probe sequences for ACO and CPT-1 (Chakravarthy et al., 2005). RT-PCR for ChPT1 and

CEPT1 was performed using the following primer-probe sets: ChPT1 (Forward, 5'-TGCTCATCTTCTACTGCCCTACAG-3'; Reverse, 5'-AGAGTCCCAGGGCACA-TAAAAG-3'; Probe, 5'-CACGGAGGAGGCACCATACTGGACAT-3'); CEPT1 (Forward, 5'-TGCTGGACGGTCCCTTCTC-3'; Reverse, 5'-ATCCATGAGGGTA-CTCTTCCAACT-3'; Probe, 5'-CCCTTAATGCAAGGATACTGGGAATGGC-3'). RNA not subjected to reverse transcription was included in each assay as a negative control. PCR reactions were performed in triplicate using an Applied Biosystems 7700 instrument. Relative mRNA levels were calculated using both the comparative C_T and standard curve methods normalized to ribosomal protein L32, an invariant internal control. Amplified bands were sequenced to verify their identity.

SDS-PAGE and Immunoblotting

Cell and tissue lysates were prepared by homogenization in a modified RIPA buffer containing a cocktail of protease and phosphatase inhibitors (Chakravarthy et al., 2005). 25 μg of total protein or an aliquot of the FLAG-eluted protein/lipid mixture was resolved by SDS/PAGE (10% polyacrylamide). Gels were stained with GelCode Blue Protein stain (Thermo Scientific), a highly sensitive Coomassie G-250-based protein stain, for 1 h followed by destaining in ultrapure water for 4 h. Other gels were transferred onto PVDF membranes (Millipore Corp.), and blotted using the following antibodies: FAS (1:1000, Abcam), FLAG M2 monoclonal antibody (1:2000, Sigma), PPARα (1:750, Santa Cruz), actin (1:5000, Sigma), and PCNA (1:1000, Cell Signaling), followed by appropriate secondary antibody incubation at 1:5000-1:7500 dilution, and detection by chemiluminescence (ECL kit, Amersham).

Histology

Livers were frozen in Tissue-Tek OCT and 5-10 μm sections were cut using a cryostat. Sections were placed on glass slides and subjected to immunofluorescence microscopy for GFP, or stained with Oil Red O (Sigma) to detect neutral lipids. Images were captured though a Nikon Eclipse E600 microscope attached to a Photometrics CoolSnap digital camera.

Establishing Conditions for Portal Vein infusion of 16:0/18:1-GPC

Small doses of fatty acids even for a short duration can exert striking metabolic effects. For example, portal venous infusion of oleate at 150 nmol/min for just 24 h induces hypertension and decreases insulin sensitivity (Benthem et al., 2000). Given the relatively high flow rate (1.5 ml/min) in the portal vein (Grekin et al., 1995), injection into this vessel leads to a direct and short transit time into the liver, thereby minimizing binding of lipids by albumin.

There are few studies regarding the specific use of phosphatidylcholine (PtdCho) infusions. In humans, PtdCho was given either intravenously at a total dose of 2 g/day for 3 days (Cantafora et al., 1992) or orally at a total dose of 2 g/day for 12 wks (Stremmel et al., 2007). In rats, PtdCho was infused at a rate of 9 μmol/h into the duodenum for 6 h (= 40 mg) (Mansbach and Dowell, 1993). We are not aware of studies that report PtdCho infusion directly into the portal vein.

We therefore extrapolated the doses in mice taking into account the direct intraportal route, and tested doses ranging from 0.1 mg/day to 10 mg/day based on a 25 g mouse. We found that rapid infusion (< 1 min) was optimal and that the lowest dose causing increased expression of the PPARα target gene acyl-CoA oxidase was 10 mg/kg. Larger doses and slower infusion rates resulted not only in poor solubility but also death due to portal vein thrombosis. Optimal

dosing frequency was determined based on kinetic data obtained by injection of ^{14}C-labeled 16:0/18:1-GPC (American Radiochemicals, St. Louis) into the portal vein of C57/BL6 mice as shown in Supplemental Fig. 7. Following a single injection into the portal vein (1.9 μCi/mouse), total counts from both cytoplasmic and nuclear fractions were obtained (Supplemental Fig. 7A). Using standard pharmacokinetic equations (Hardman et al., 2001), a dosing interval of 8.7 hours was calculated, indicating an optimal dosing frequency of three times a day.

Maximum recovery of the injected ^{14}C-labeled compound ranged from 10-15% of the total injected dose in nuclear fractions (Supplemental Fig. 7B). While it is possible that the recovered counts might not represent the intact 16:0/18:1-GPC molecule, indirect evidence in Caco-2 cells suggests that labeled PtdCho is not rapidly hydrolyzed (Treede et al., 2007). Assuming that the PtdCho species injected into the portal vein of mice remained stable for 30 min, peak nuclear recovery exceeds that seen in Caco2 cells (Treede et al., 2007). This likely represents a pharmacological dose because 16:0/18:1-GPC is a minor phosphatidylcholine species in liver (Hsu et al., 1998).

Supplemental References

Benthem, L., Keizer, K., Wiegman, C.H., de Boer, S.F., Strubbe, J.H., Steffens, A.B., Kuipers, F., and Scheurink, A. (2000). Excess portal venous long-chain fatty acids induce syndrome X via HPA axis and sympathetic activation. Am J Physiol Endocrinol Metab *279*, E1286-E1293.

Bernal-Mizrachi, C., Weng, S., Feng, C., Finck, B.N., Knutsen, R.H., Leone, T.C., Coleman, T., Mecham, R.P., Kelly, D.P., and Semenkovich, C.F. (2003). Dexamethasone induction of hypertension and diabetes is PPARalpha-dependent in LDL receptor-null mice. Nat Med *9*, 1069-1075.

Cantafora, A., Masella, R., Angelico, M., Gandin, C., Blount, R.J., and Peterson, S.W. (1992). Effect of intravenous polyunsaturated phosphatidylcholine infusion on insulin receptor processing and lipid composition of erythrocytes in patients with liver cirrhosis. Eur J Clin Invest *22*, 777-782.

Chakravarthy, M.V., Pan, Z., Zhu, Y., Tordjman, K., Schneider, J.G., Coleman, T., Turk, J., and Semenkovich, C.F. (2005). "New" hepatic fat activates PPARalpha to maintain glucose, lipid, and cholesterol homeostasis. Cell Metab *1*, 309-322.

Grekin, R.J., Vollmer, A.P., and Sider, R.S. (1995). Pressor effects of portal venous oleate infusion: a proposed mechanism for obesity hypertension. Hypertension *26*, 193-198.

Hardman, J.G., Limbird, L.E., and Gilman, A.G.E. (2001). Goodman & Gilman's The Pharmacological Basis of Therapeutics (McGraw Hill).

Hsu, F.F., Bohrer, A., and Turk, J. (1998). Formation of lithiated adducts of glycerophosphocholine lipids facilitates their identification by electrospray ionization tandem mass spectrometry. J Am Soc Mass Spectrom *9*, 516-526.

Mansbach, C.M., and Dowell, R.F. (1993). Portal transport of long acyl chain lipids: effect of phosphatidylcholine and low infusion rates. Am J Physiol *264*, G1082-G1089.

Shi, Y., Hon, M., and Evans, R.M. (2002). The peroxisome proliferator-activated receptor delta, an integrator of transcriptional repression and nuclear receptor signaling. Proc Natl Acad Sci USA *99*, 2613-2618.

Stremmel, W., Ehehalt, R., Autschbach, F., and Karner, M. (2007). Phosphatidylcholine for steroid-refractory chronic ulcerative colitis: a randomized trial. Ann Intern Med *147*, 603-610.

Tordjman, K., Standley, K.N., Bernal-Mizrachi, C., Leone, T.C., Coleman, T., Kelly, D.P., and Semenkovich, C.F. (2002). PPARalpha suppresses insulin secretion and induces UCP2 in insulinoma cells. J Lipid Res *43*, 936-943.

Treede, I., Braun, A., Sparla, R., Kuhnel, M., Giese, T., Turner, J.R., Anes, E., Kulaksiz, H., Fullekrug, J., Stremmel, W.*, et al.* (2007). Anti-inflammatory effects of phosphatidylcholine. J Biol Chem *282*, 27155-27164.

Supplemental Table 1: Liver function studies

Liver function	CHOW						ZFD					
	WT/PPARα$^{-/-}$			FASKOL/PPARα$^{-/-}$			WT/PPARα$^{-/-}$			FASKOL/PPARα$^{-/-}$		
	Saline (n =3)	AdGFP (n =6)	AdPPARα (n= 5)	Saline (n =3)	AdGFP (n= 6)	AdPPARα (n= 5)	Saline (n =3)	AdGFP (n= 5)	AdPPARα (n= 6)	Saline (n =3)	AdGFP (n= 6)	AdPPARα (n= 6)
ALT (IU/L)	32.0 ± 12.2	36.1 ± 10.2	39.5 ± 7.2	33.3 ± 9.1	38.5 ± 11.1	40.8 ± 9.4	32.1 ± 9.3	35.1 ± 6.9	38.7 ± 8.5	34.1 ± 11.5	43.7 ± 8.7	42.1 ± 9.6
Alkaline phosphatase (IU/L)	88 ± 5.2	86 ± 3.2	92 ± 7.3	87 ± 3.2	81 ± 4.1	83 ± 6.2	84 ± 4.2	94 ± 11.0	85 ± 4.0	87 ± 3.6	88 ± 6.5	89 ± 7.3
Total bilirubin (mg/dL)	0.33 ± 0.4	0.37 ± 0.1	0.28 ± 0.09	0.31 ± 0.1	0.30 ± 0.07	0.27 ± 0.06	0.32 ± 0.2	0.36 ± 0.07	0.32 ± 0.04	0.30 ± 0.3	0.37 ± 0.11	0.29 ± 0.09
Albumin (g/dL)	3.2 ± 0.4	3.1 ± 0.2	3.5 ± 0.6	3.1 ± 0.3	2.8 ± 0.1	3.3 ± 0.2	3.0 ± 0.3	2.9 ± 0.1	3.2 ± 0.2	3.4 ± 0.4	3.3 ± 0.1	3.0 ± 0.2

Male mice (16-20 wks) were maintained on chow or were fed zero-fat diet (ZFD) for a week. Four days after receiving an intravenous injection of either normal saline or the indicated adenoviruses (8.5×10^{10} PFU), and immediately before harvesting tissues, blood samples were obtained. Each value represents the mean ± SEM.

Supplemental Table 2: Nuclear GPC concentrations

GPC Species	Fed	Fasted
16:0/18:1	7.87 ± 1.3	8.03 ± 0.80
16:0/18:2	23.7 ± 3.5	30.5 ± 2.8
18:1/18:1	11.7 ± 2.0	8.95 ± 0.84

Nuclear fractions were prepared from livers of mice in the fed state and after 20 hours of fasting. Data are expressed as mean ± SEM in units of pmol GPC species/μg nuclear protein for 9 mice in the fed state and 9 mice in the fasted state. These animals were studied in 3 independent experiments involving 3 animals per condition over the span of several weeks.

For these assays, nuclear aliquots containing 50 mg of protein were placed in borosilicate test tubes, and methanol (2 mL), chloroform (2 mL), and aqueous LiCl (1.8 mL of 50 mM) were added. Aliquots of internal standard solutions were added, the mixtures were vortex-mixed and centrifuged, and the lower (chloroform-containing) layer was removed. The upper layer was extracted again with chloroform (2 mL), and the mixture was vortex-mixed and centrifuged again. The lower phase was combined with that from the first extraction step and concentrated to dryness under nitrogen. The residue was reconstituted in chloroform/methanol, mixed with aqueous LiCl, vortex-mixed, and centrifuged. The lower phase was removed and concentrated to dryness under nitrogen. The residue was reconstituted in chloroform/methanol containing LiCl to achieve a final volume of 500 μL per mg of starting nuclear protein, and the lipid phosphorus content of an aliquot of the extract was measured so that the contribution of individual species to total nuclear phospholipid could be calculated. GPC species were analyzed as Li^+ adducts by positive ion ESI/MS. For tandem MS, precursor ions selected in the first quadrupole were accelerated into a chamber containing argon and product ions were analyzed in the final quadrupole. MS data were automatically processed by the LipidQA program, which compares intensities of ions for internal standards to those of ions for endogenous species with a subtraction deisotoping algorithm followed by interpolation from calibration curves.

Chakravarthy et al.

Supplemental Fig. 1

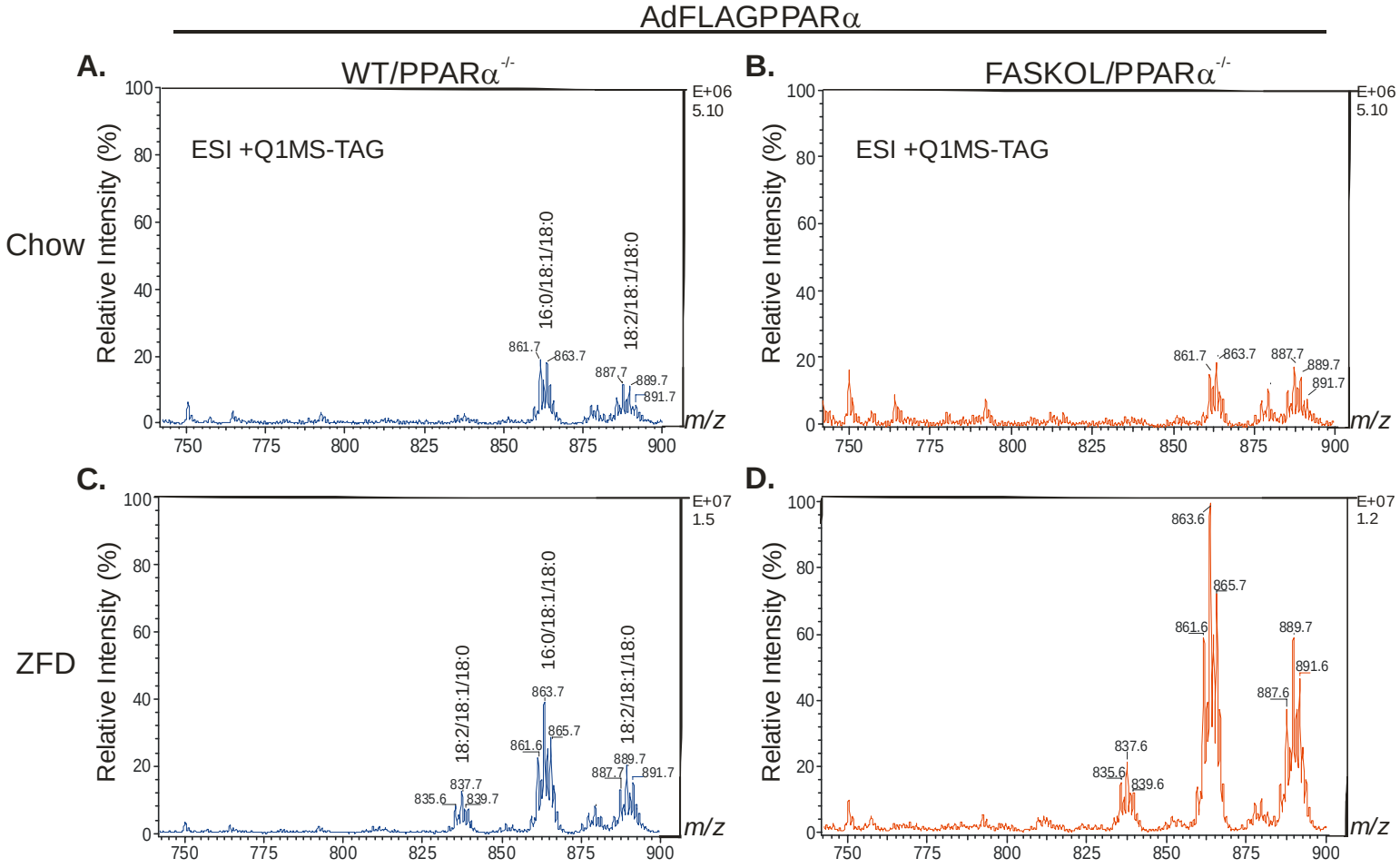

Supplemental Fig 1. Representative positive ion (+Q1) ESI/MS analyses of triacylglycerol (TAG) species in the excess FLAG-eluted hepatic nuclear extracts obtained from either chow- (**A** and **B**) or zero fat diet (ZFD) (**C** and **D**) fed WT and FASKOL mice on a PPARα null background infected with the AdFLAG-PPARα adenovirus. The mass-to-charge (*m/z*) ratios denote the molecular identity of the corresponding TAGs in each peak cluster.

Chakravarthy et al.
Supplemental Fig. 2

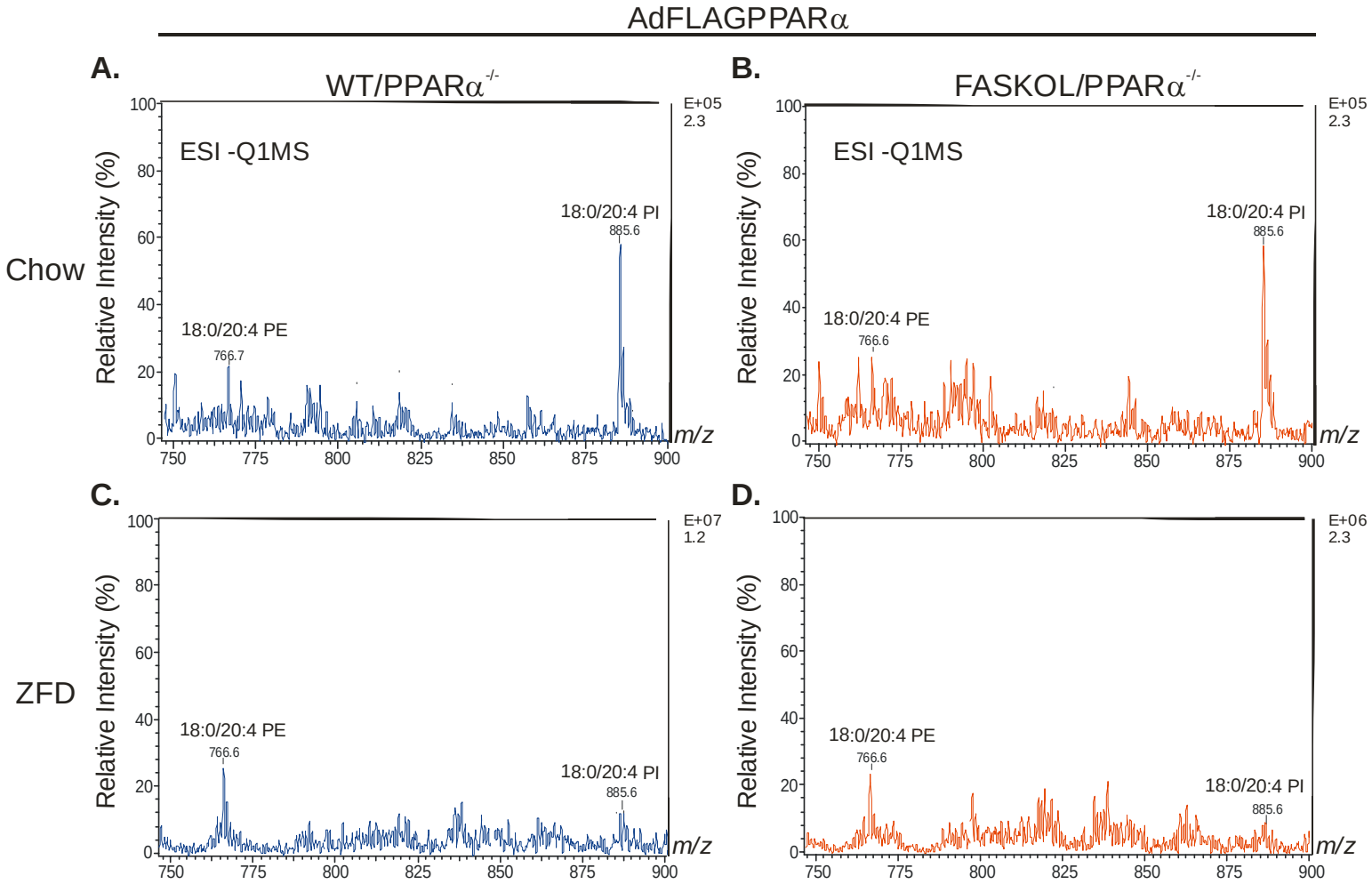

Supplemental Fig 2. Representative negative ion (-Q1) ESI/MS analyses of nuclear phospholipids in the excess FLAG-eluted hepatic nuclear extracts obtained from either chow- (**A** and **B**) or zero fat diet (ZFD) (**C** and **D**) fed WT and FASKOL mice on a PPARα null background infected with the AdFLAG-PPARα adenovirus. The fragment ion at *m/z* 766 and 885 depict 18:0/20:4 phosphatidylethanolamine (PE) and phosphatidylinositol (PI), respectively.

Chakravarthy et al.

Supplemental Fig. 3

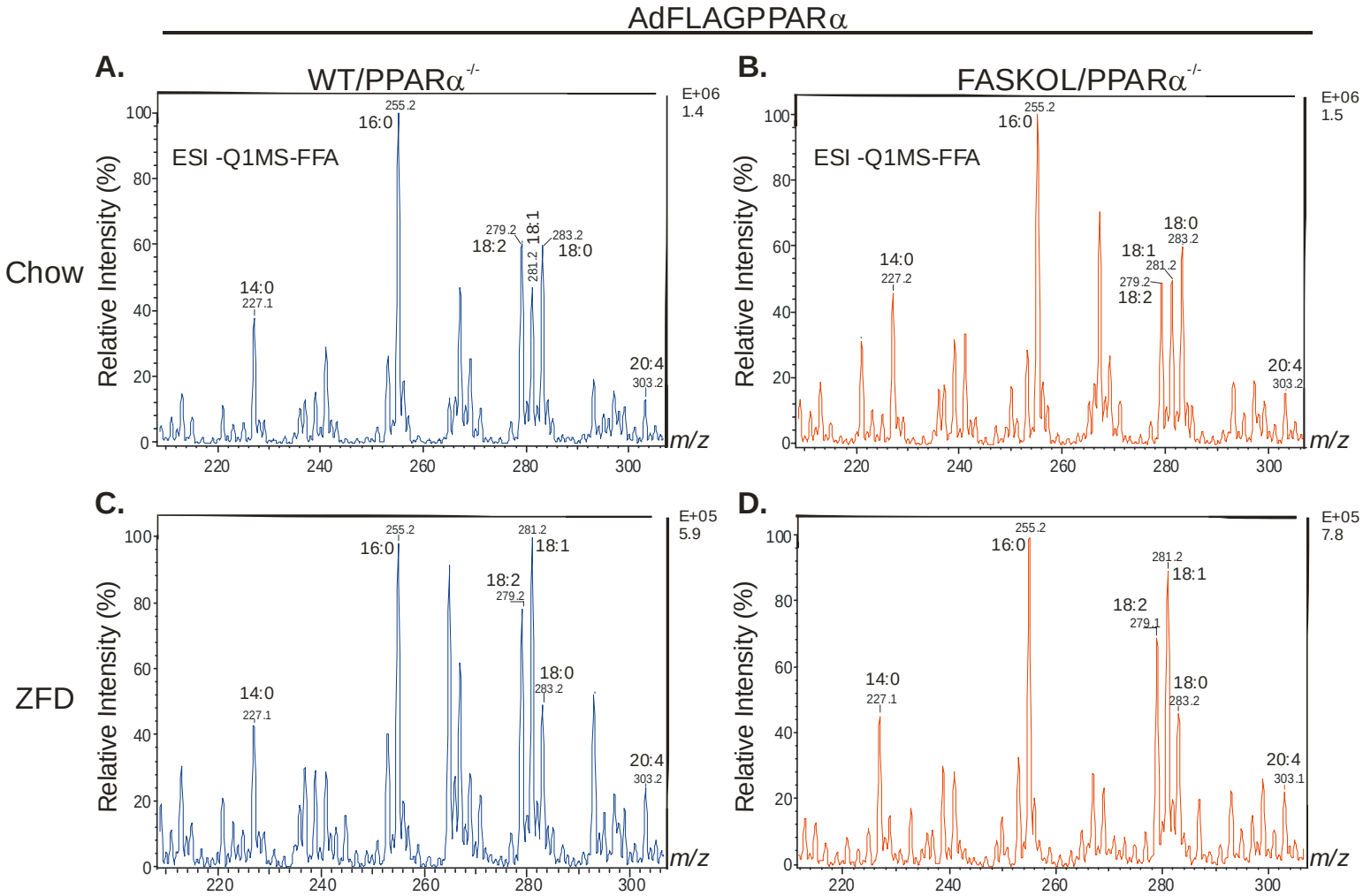

Supplemental Fig 3. Representative negative ion (-Q1) ESI/MS analyses of nuclear free fatty acids (FFA) in the excess FLAG-eluted hepatic nuclear extracts obtained from either chow- (**A** and **B**) or zero fat diet (ZFD) (**C** and **D**) fed WT and FASKOL mice on a PPARα null background infected with the AdFLAG-PPARα adenovirus. Fatty acids are identified by their corresponding *m/z* ratios as depicted in each of the profiles.

Chakravarthy et al.
Supplemental Fig. 4

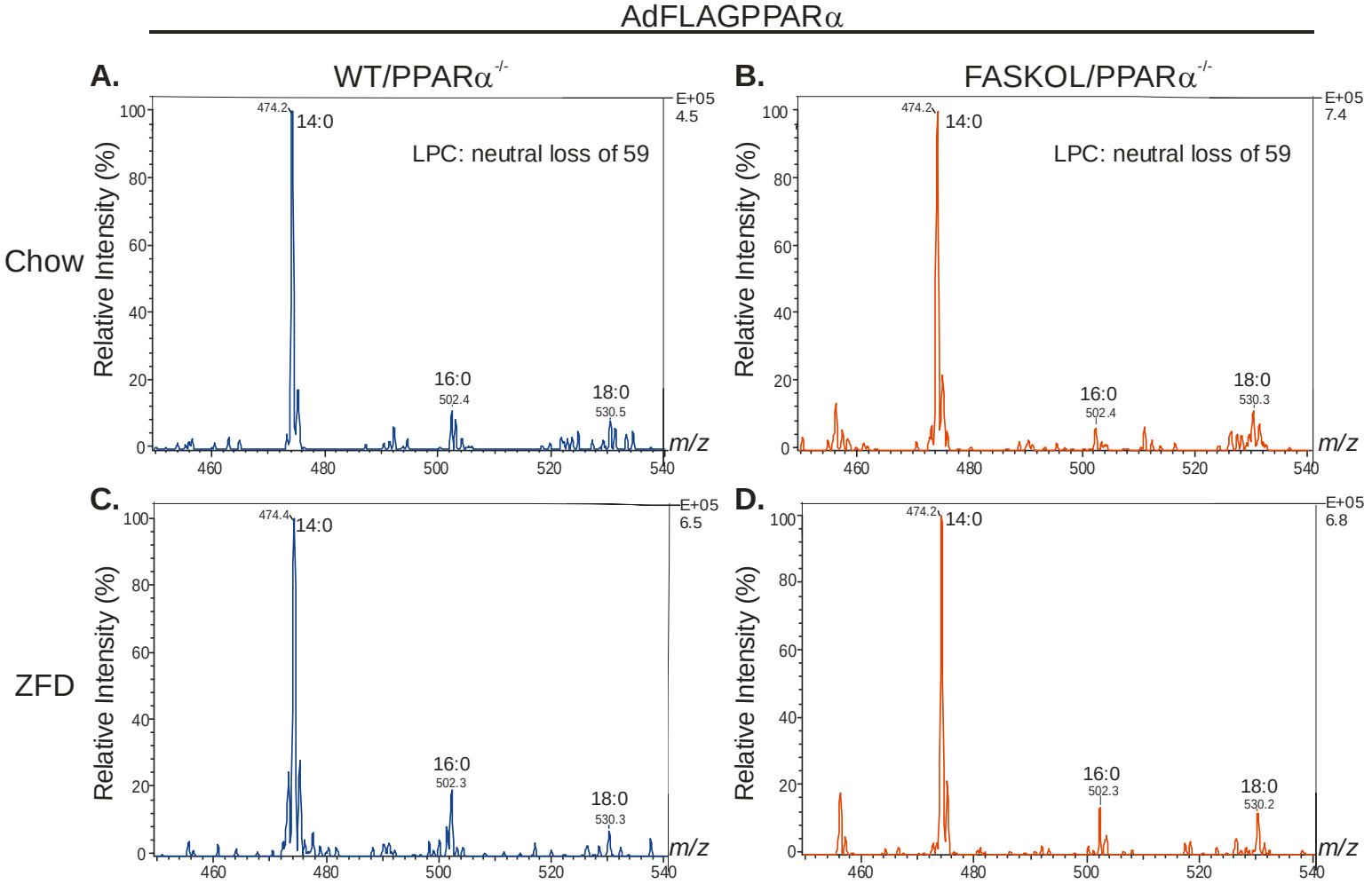

Supplemental Fig 4. Positive ion ESI/MS analyses of lithiated adducts of hepatic nuclear phospholipids were performed to monitor neutral loss of 59 [$N(CH_3)_3$], which identifies parent ions that contain the lysophosphatidylcholine (LPC) head-group in the excess FLAG-eluted hepatic nuclear extracts obtained from either chow- (**A** and **B**) or zero fat diet (ZFD) (**C** and **D**) fed WT and FASKOL mice on a PPARα null background infected with the AdFLAG-PPARα adenovirus. The fatty acid moieties in LPC are identified by their corresponding *m/z* ratios as depicted in each of the profiles.

Chakravarthy et al.

Supplemental Fig. 5

A.

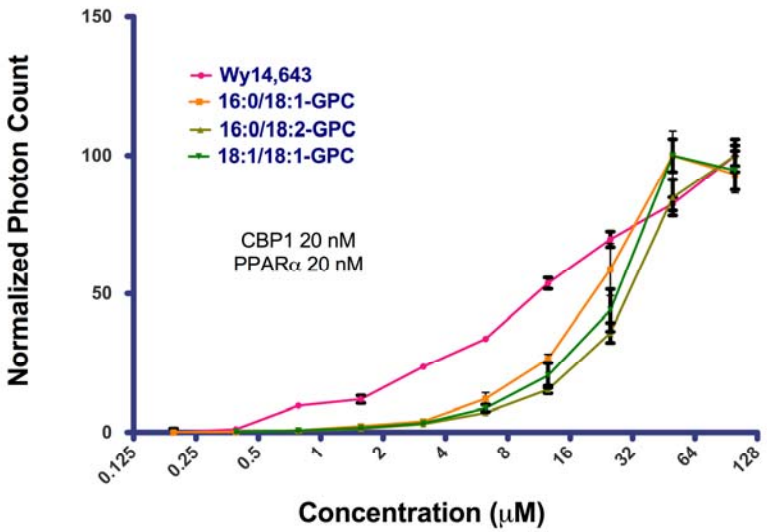

B.

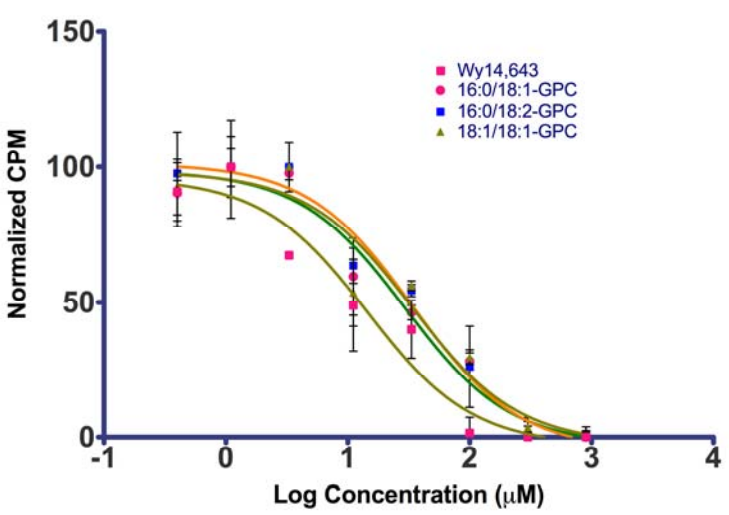

C.

	Wy14,643	16:0/18:1-GPC	16:0/18:2-GPC	18:1/18:1-GPC
IC50	11.12(±0.33)	33.25(±0.29)	33.40(±0.30)	33.47(±0.34)
Ki	11.06(±0.33)	33.20(±0.29)	33.35(±0.30)	33.41(±0.34)

Supplemental Fig 5. Determination of relative binding affinities of GPC species. **A**. Relative affinity was assessed by Alpha Screen assay using the PPARα LBD , the co-activator peptide CBP1, and increasing concentrations of ligand. **B**. Affinity was also determined by scintillation proximity assay using ^{3}H-Wy14,643 (1.25 μM), H6 GST PPARα LBD (150 nM) and increasing concentrations of cold ligand for displacement. The buffer composition was 50 mM MOPS, 50 mM NaF, 0.05 mM CHAPS, 5.0 mg/ml BSA (pH 7.4). Ligand concentrations were 900, 300, 100, 33.3, 11.1, 3.7, 1.23 and 0.41 μM. IC50 and Ki values (mean ± SEM) are shown in **C**.

Chakravarthy et al.

Supplemental Fig. 6

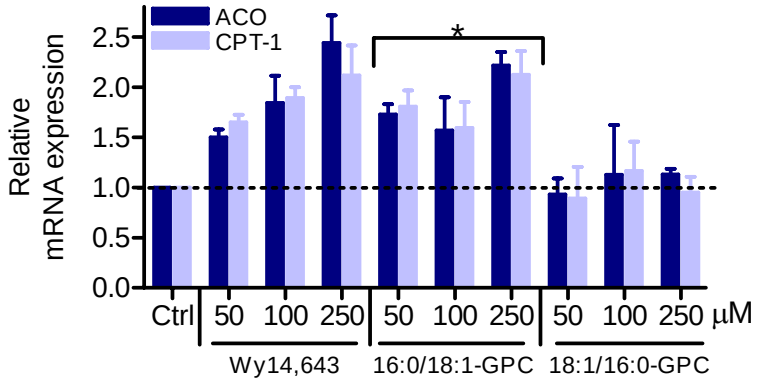

Supplemental Fig 6. Effect of Wy14,643, 16:0/18:1-GPC, and 18:1/16:0-GPC on PPARα target gene (ACO and CPT-1) expression by quantitative RT-PCR in Hepa 1-6 cells treated for 24 h. Results are mean ± SEM of 9 separate experiments. *, $P < 0.05$ compared to control (Ctrl, 80% PBS/20% DMSO).

Chakravarthy et al.

Supplemental Fig. 7

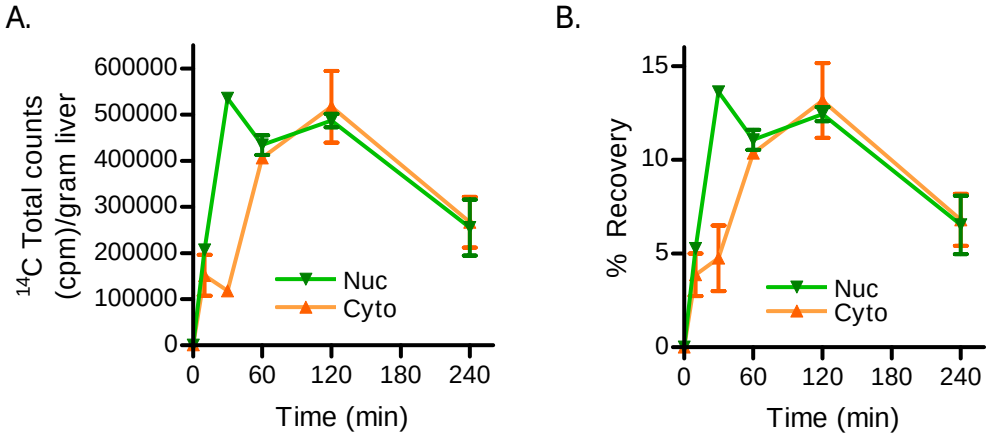

Supplemental Fig 7. Kinetic assays for ^{14}C-16:0/18:1-GPC. After a single intraportal injection of the radiolabeled GPC (1.9 μCi/mouse sonicated to homogeneity in a 37ºC solution of normal saline/0.5% ethanol/0.5% fatty acid-free BSA), livers were harvested at the indicated times, and their cytosolic and nuclear fractions were prepared . Lipids were extracted in each of these fractions and the corresponding counts were measured and were normalized to tissue weight (**A**). Recovery of the radiolabel was calculated based on the counts obtained at the indicated times normalized to total counts injected per gram of liver (**B**). Graphs represent mean **±** SEM of 3 separate experiments with 3-4 mice per group.